Proceedings of the
International Conference on Mechanical Engineering and Renewable Energy 2011
(ICMERE2011) 22- 24 December 2011, Chittagong, Bangladesh

ICMERE2011-PI-187

ASSESSMENT OF CLOSED-TEST-SECTION WIND TUNNEL BLOCKAGE USING CFD

Prasanjit Das*[1], **A.S.M. Sayem**[2], **Tilok Kumar Das**[3] and **A.K. Azad**[4]

[1] Hokkaido University, Sapporo, Hokkaido, Japan
[2,3]CUET, Dept. of Mechanical Engineering., Bangladesh
[4]University of Chittagong, Dept. of Physics, Bangladesh
prasanjitd11@yahoo.com*, yessayem@yahoo.com, tilok_cuet@yahoo.com, kalamphysics@yahoo.com

Abstract*- The wind tunnel interference (blockage) effects in closed-test-section wind tunnel were investigated using CFD (Computational fluid dynamics) simulations. Flow over full-scale heavy duty truck model representing one of the most freight transportation vehicles was analyzed. The model was placed at different yaw angles between 0 to 10 degrees in two different virtual wind tunnels with blockage ratio of about 10% and 1%; reflect the aerodynamic drag coefficient at blockage (baseline) and blockage free (ideal) condition respectively. From simulations, first we calculated the increment of aerodynamic drag coefficient (ΔC_d) between baseline and ideal condition. Then the corrected drag coefficient was determined depending on the correction of dynamic pressure ratio (q_c/q) for solid and wake blockage by several existing blockage correction equations. We have also searched for the best correction equation for the blockage effect in order to obtain ideal drag coefficient. A CFD based blockage correction method is proposed.*

Keywords: Wind-Tunnel Blockage, Closed-test-section Wind-Tunnel, Dynamic Pressure Correction

1. INTRODUCTION

While road testing is the most accurate method for assessing a vehicle's aerodynamic performance, there are difficulties associated with the ever-changing wind conditions. Alternative to road testing, from over a century, the aerodynamic performance of road vehicles has mainly assessed by the wind tunnel measurements. The capital required for the development of experimental facilities, such as aerodynamic wind tunnels is very high. Not only the experimental procedure is very time consuming, but also there is an increasing demand for reliable wind tunnel data, and so developmental costs are rising steeply. The accuracy of drag coefficients reported by various groups of researchers was achieved only through a costly and tedious process of preparing a full-scale model and then conducting tests on it. The wind tunnel is an ideal indispensible tool for aerodynamic development because it enables the measurement of aerodynamic forces and moments. Although actual full-scale automotive vehicles can be tested, the realism of such simulations is limited by the finite size of the test section, the complexities of the moving ground rigs. Moreover, the results for scale model tests are subjected to numerous doubts associated with the effect of the Reynolds number (Re), the fidelity of the model, the absence of the engine cooling and passenger compartment flows, the lack of under hood and under body details, the effect of the tunnel wall boundary layer, the effects of model support interference, and the effects of flow-intrusive probes. The most important factor to be addressed in wind tunnel testing is the effect of blockage, which results from the presence of closed wall boundaries around the vehicle that affect the measured aerodynamic properties. The blockage effects imposed by the walls of a wind tunnel distort the flow field round a model so that the test result does not give an actual representation of conditions in an unconfined flow. Therefore, correction is needed before the measured result can represents the vehicle's performance under actual road condition, which is free from the wall constraint (blockage) effects.

To surmount some of the difficulties associated with wind tunnel testing and on-road measurement, wind tunnel experts and researchers have invented computerized flow simulation techniques. Many mathematical techniques and flow models emerged in the early 1970s that provide better and more efficient algorithms related to fluid flow simulation. Increases in computer capacity and advances in computational technologies enabled the development of computational fluid dynamics, a strong alternative numerical tool for determining vehicle aerodynamic forces and moments. Recent advances in high-performance computing techniques have reduced the cost and time of CFD analysis considerably. The use of CFD analysis has several advantages over wind tunnel experiments and on-road measurements: it is quicker due to the high computational speeds of modern super computers, it provides detailed information about the flows for both the spatial and time dimensions, and there are no scaling

effects. Moreover, it can be used for validating wind tunnel test results.

The purpose of the present study is to investigate the closed-test-section wind tunnel blockage effect on full-scale heavy truck by using CFD, to assess the blockage correction equations for real vehicle model, and proposed the CFD based correction for blockage free aerodynamic drag.

2. NUMERICAL METHODS

2.1 Governing Equations and Discretization:

An incompressible Newtonian fluid was assumed, and continuity and momentum equations were spatially filtered to obtain the governing equations of LES:

$$\frac{\partial \overline{u}_i}{\partial x_i} = 0 , \quad (1)$$

$$\frac{\partial \overline{u}_i}{\partial t} + \frac{\partial}{\partial x_j}\overline{u}_i\overline{u}_j = -\frac{\partial \overline{P}}{\partial x_i} + 2\frac{\partial}{\partial x_j}\left(\nu + \nu_{SGS}\right)\overline{S}_{ij} , \quad (2)$$

The bar over the physical quantity indicates the spatial filtering operation for LES. The filtered strain rate tensor $\overline{S}_{ij}$ and pressure $\overline{P}$ in Eq. (2) are expressed as

$$\overline{S}_{ij} = \frac{1}{2}\left(\frac{\partial \overline{u}_j}{\partial x_i} + \frac{\partial \overline{u}_i}{\partial x_j}\right) , \quad (3)$$

$$\overline{P} = \overline{p}/\rho + \left(\overline{u_i u_j} - \overline{u}_i\overline{u}_j\right)/3 , \quad (4)$$

In Eq. (2), the last term on the right represents the effect of subgrid-scale (SGS) turbulence, which was modeled under the eddy viscosity assumption. The conventional Smagorinsky model (Smagorinsky, 1963) was used, and the eddy viscosity coefficient was modeled as

$$\nu_{SGS} = \left(C_s f_d \Delta\right)^2 \sqrt{2\overline{S}_{ij}\overline{S}_{ij}} , \quad (5)$$

where Δ is the length scale of the SGS turbulence expressed as the cube root of each numerical mesh, and model coefficient C_s is set to 0.15, which is generally suitable for external flows. The damping of the turbulent effect near a wall boundary is explained by the Van-Driest type damping function as follows:

$$f_d = 1 - \exp\frac{-l^+}{25} , \quad (6)$$

where l^+ is the distance from the wall in wall coordinates.

The governing equations were discretized by using the vertex-centered unstructured finite volume method. The second-order central differencing scheme was applied for the spatial derivatives and blending of 5% first-order upwind scheme for the convection term was employed for numerical stability. The third-order upwind scheme was adopted for the spatial derivative far away from vehicle, where coarser grid was allocated. For time marching, the third-order Adams-Moulton semi-implicit scheme was used. Pressure-velocity coupling was preserved by using the Simplified Marker and Cell (SMAC) algorithm. The pressure Poission equation was solved by the incomplete Cholesky conjugate gradient (ICCG) method.

2.2 Target Vehicle Model:

The configuration of the full-scale heavy-duty truck model is shown in Fig. 1.The surface of the vehicle is reproduced by about 1.5 million triangle meshes. To reproduce the fine structure, the surface resolution is around 5 to 10 mm around the side mirror, and relatively fine elements are allocated around the cabin.

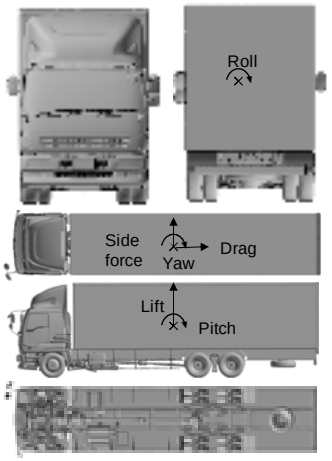

Fig. 1: Full-scale heavy-duty truck

(a)

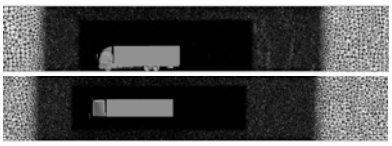

(b)

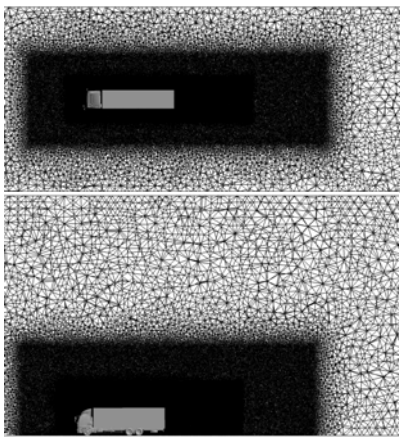

Fig. 2: Spatial elements around the model with the air deflector at 0° yaw angle (a) Baseline case (b) ideal case

The engine and power train is reproduced by the

moderate elements with the resolution of 20 to 50 mm. Larger elements are allocated to reproduce the cargo panel. The fluid space was decomposed by tetrahedral elements. To maintain finer resolution around the vehicle, hierarchical allocation is carried out as shown in Fig. 2.

2.3 Computational Domain and Boundary Condition

In the computational analysis conducted to assess the closed-wall wind tunnel blockage, two different virtual wind tunnels were considered. They are baseline virtual wind tunnel for which the blockage effect is to be found. The baseline virtual wind tunnel with its test section of 9.5 by 9.5 meters is shown in Fig. 3(a), blockage ratio about of 10% corresponds to the DNW-German Dutch wind tunnel.

In the real road condition, blockage effect does not exist. To simulate such a condition, we created a numerical domain with its test section of 32.4 by 25.0 meters in order to negligible blockage ratio. Hence, we termed this condition an idea condition, which has the blockage ratio of around 1%, as shown in Fig. 3(b).

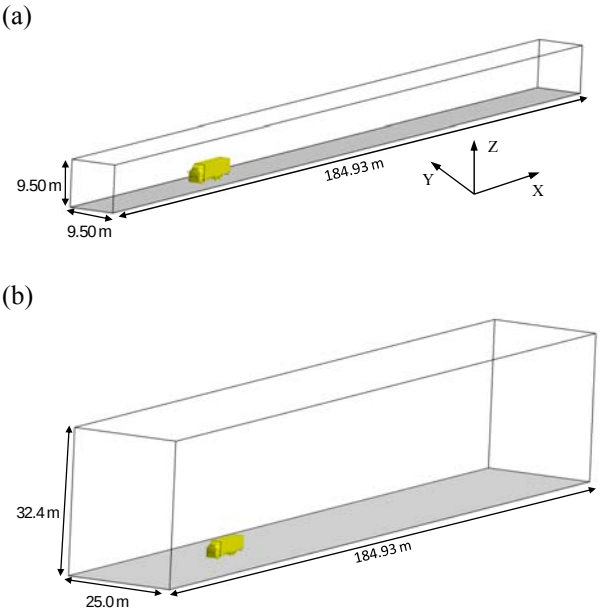

Fig. 3: Computational domains: (a) Baseline case, (b) Ideal case

In both cases, a uniform velocity distribution U_0 is defined at the inlet (about 22 m/s and 25 m/s in the real wind tunnel and ideal cases, respectively) about 40 m upstream of the vehicle. All velocity components were gradient-free for the steamwise direction at the outlet. Solid wall condition was adopted on the surface of the vehicle body and the floor on which the vehicle was mounted. It was impossible to resolve the entire boundary layer at a reasonable computational cost, especially in the vicinity of the solid wall where large velocity gradient appears. The log-law profile was assumed on the velocity and surface friction on the wall was estimated and directly imposed as Neumann boundary condition. As a result of the assumed log-law profile, the first nearest grid point was allocated so as to maintain the distance from the wall less than about 200 in wall unit (y+), which are located within the logarithmic layer of the boundary layer.

3. REEVIEW OF WIND-TUNNEL BLOCKAGE CORRECTION EQUATIONS

It is defined that the total blockage correction factor is the sum of velocity acceleration (blockage factor) caused by solid and wake blockage; however these are more difficult factors to assess for unusual geometries such as the heavy-duty truck with including complicated detail characteristics features and the associated flow fields around them.

The continuity correction [1] scheme accounts only solid blockage and was based only upon the geometric reduction in test section area due to the presence of the model. The corrected dynamic pressure is then expressed by the following relation:

$$\frac{q_c}{q} = \left[1 - \left(\frac{A_M}{A_N}\right)\right]^{-2}, \tag{7}$$

This roughly corresponds to the following blockage correction coefficient:

$$\varepsilon \approx \frac{A_M}{A_N}, \tag{8}$$

The area ration method [1] was also based upon purely geometric considerations but is meant to account for both solid and wake blockage in a single geometric term. It is suggested by Barlow, Rae, and Pope for blockage estimates *"when all is lost as far as finding blockage corrections for some unusual shape"* [1].The suggested form for the blockage correction coefficient is as follows:

$$\varepsilon \approx \frac{1}{4}\frac{A_M}{A_N}, \tag{9}$$

Resulting in the following relation:

$$\frac{q_c}{q} = \left[1 - \frac{1}{4}\left(\frac{A_M}{A_N}\right)\right]^{2}, \tag{10}$$

The empirically derived [2] wall proximity method is a boundary interference correction method that accounts for the presence of side walls and a ceiling near the test model. This method was empirically derived and is applicable to the particular vehicle shapes, drag levels, and specific wind tunnel geometry.

$$C_D = C'_D - \left(\frac{dC_D}{db_r}\right)b_r - \left(\frac{dC_D}{db_r}\right)h_r, \tag{11}$$

Thom [6] had developed blockage correction based on classical work of Glauert and Lock that facilitate to apply for streamlined body, attached-flow bodies in

closed-test-section tunnels of various cross-sectional shapes. Herriot [1] also expanded expressed in the form of dynamic pressure is as:

$$\frac{q_c}{q} = \left[1 + T\left[\frac{V}{C^{3/2}}\right] + \frac{1}{4}C_{D_{uw}}\left(\frac{A_M}{A_N}\right)\right]^2, \quad (12)$$

Maskell [3] was the first to address the problems with non-streamline flow bodies, such as bluff-body testing in closed-wall wind tunnel. Maskell's theory is derived on the basis that the test specimen (i.e. circular flat plate) was located at the center of the test section. The correction of the dynamic pressure ratio is as follows:

$$\frac{q_c}{q} = \left[1 + \frac{5}{2}C_{D_{uw}}\left(\frac{A_M}{A_N}\right)\right], \quad (13)$$

$$C_{D_w} = C_{D_{uw}} / \left(q_c / q\right), \quad (14)$$

where q_c is corrected dynamic pressure, q is uncorrected dynamic pressure, A_M is flat plate area, and A_N is wind tunnel working section cross sectional area.

Maskell's momentum analysis combined the dynamic pressure and the incremental drag blockage components into a single dynamic pressure adjustment, making it a correction to drag only. Hackett then re-correct the blockage correction in terms of a blockage-induced increment velocity and a drag increment, to produced the following two-step (dynamic pressure and incremental drag) correction,

$$C_{DcM2} = \frac{\left(C_{Du} + \Delta C_{DM}\right)}{\left(q_c / q\right)}, \quad (15)$$

where, C_{DcM2} is wind-axis drag coefficient corrected by Hackett's two-step version of Maskell, eqn. (15)

$$\Delta C_{DM} = \frac{C_{Du}}{\left(1 + \frac{5}{2}C_{Du}\frac{A_M}{A_N}\right)} + \left[\frac{C_{Du}}{2.\frac{5}{2}C_{Du}\frac{A_M}{A_N}}\right] \left[1 - \left(1 + 4.\frac{5}{2}C_{Du}\frac{A_M}{A_N}\right)^{1/2}\right], \quad (16)$$

where, ΔC_{DM} is drag increment due to separated-flow wake constraint.

Mercker [3] provides a blockage correction equation based on the work of Lock [5] for solid blockage and on the work of Maskell [2], Thom [6], and Glauert [7] for wake blockage. Mercker's correction considers the effects of yaw angle, vehicle geometry, and wind tunnel geometry. The correction expressed by the ratio of dynamic pressure as follow:

$$\frac{q_c}{q} = \left[1 + K_3\tau' \frac{2A_{M\psi}.2V_M}{\sqrt{L_p.2V_M.(2A_N)^{3/2}}} + \frac{2A_M}{2A_N}.\left(\frac{1}{4}C_{Dm}(0) + \eta\frac{2A_{M\psi}}{2A_N}\right)\right]^2 \quad (17)$$

where ε_s is solid blockage factor, ε_w is wake blockage factor, $A_{M\psi}$ is vehicle frontal area at ψ degree yaw angle, V_M is vehicle volume, and $C_{Dm}(0)$ is the measured drag coefficient at 0 degree yaw angle.

The drag coefficient is fully corrected in order to consider wake distortion and horizontal pressure buoyancy by

$$C_{DT} = C_{Duw} + \Delta C_{pw} + \Delta C_{DHB}, \quad (18)$$

$$C_{Dw} = C_{DT} / \left(q_c / q\right), \quad (19)$$

Wake distortion term:

$$\Delta C_{pw} = \left(C_{pwc} - C_{pmb}\right), \quad (20)$$

Drag correction due to the horizontal buoyancy is expressed as:

$$\Delta C_{DHB} = \left[1.75 / A_M\right]\left[V_M / 2\right]G, \quad (21)$$

4. RESULTS AND DISCUSSION

4.1 Empty Tunnel Simulations

In closed-test-section wind tunnel blockage correction usually consists two parts: a correction to the measured dynamic pressure (q-correction) and a gradient correction. From 4, we can see that pressure gradients were occurred over the vehicle position as well as over the wake region due to boundary layer development. The purpose of empty tunnel simulations was to discern the blockage mechanism due to non-uniform streamwise pressure gradient correction.

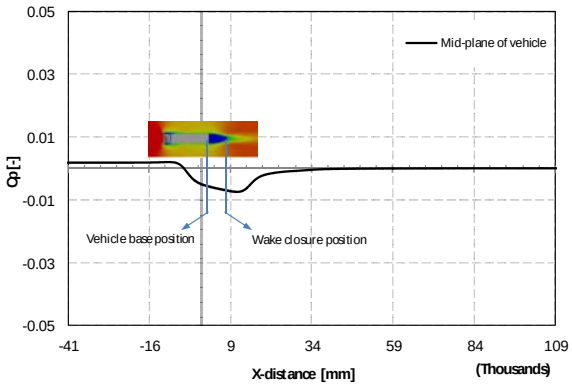

Fig. 4: Longitudinal pressure gradient for empty baseline wind tunnel

In closed-test section wind tunnel the aerodynamic drag influence by two factors, which are related to tunnel

pressure gradient. First one is horizontal buoyancy correction due to empty tunnel gradients over the model. Secondly, wind tunnel correction arising from the presence of the wake is a gradient correction to the measured drag. The two factors only considered in Mercker's method.

4.2 Wind Tunnel Blockage

As previously mentioned in the introduction section, the wind tunnel blockage effect arises because of the constraining effect of the solid walls of the wind tunnel. From Fig.5 shows that the pressure coefficient distribution on the ceiling and side walls of the baseline virtual wind tunnel when the truck model is placed in the virtual wind tunnel. The constraining effect is clearly evident, given the variations in pressure coefficient, which varies from 0 to −0.26. The pressure coefficient can be further illustrated by the Fig. 6, which shows the pressure coefficient distribution on the symmetry lines of the wind tunnel ceilings. Pressure signatures for both the baseline virtual wind tunnel and ideal condition virtual wind tunnel, are shown in Fig.6.

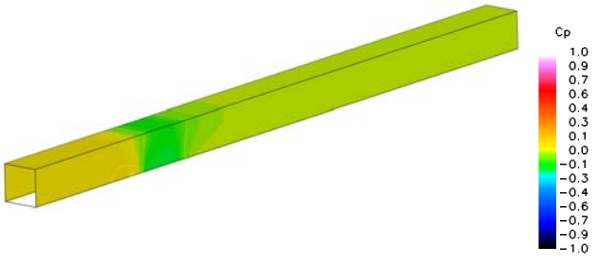

Fig. 5: Visualization of pressure signature on ceiling and side walls of baseline wind tunnel

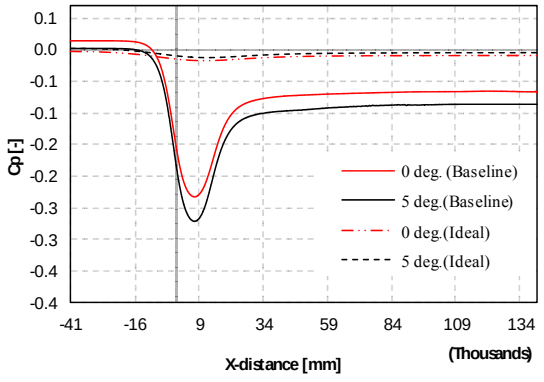

Fig. 6: Pressure coefficient distribution along symmetry lines of virtual wind tunnel ceiling (baseline wind tunnel, and ideal condition wind tunnel)

A number correction methods have been proposed and can be found in [1]. These correction methods are based mainly on potential flow theory and/or empirical correlations. The resulting blockage free aerodynamic drag coefficients and aerodynamic drag coefficients for this model in the baseline virtual wind tunnel are given in Table 1. The drag increment due to blockage effect in baseline wind tunnel is defined by following equation as

$$\Delta C_D(CFD) = C_D(Baseline) - C_D(Ideal)\,, \qquad (22)$$

In this case, it is assumed that the test is done in DNW as reflected in the choice of the baseline virtual wind tunnel. It is assumed that the blockage effect can be accurately captured in CFD. It should be mentioned that below represented drag coefficient shows as a normalized value for confidential reason, but the difference between ideal and baseline condition shows the absolute value.

Table 1: Blockage effect

Yaw angle	0°	5°	10°
$C_d\,(Ideal)$	1.000	1.136	1.365
$C_d\,(Baseline)$	1.000	1.176	1.495
$\Delta C_d\,(CFD)$	**0.132**	**0.176**	**0.266**

Evaluation of the correction methods against the available data was given in Table 1. The general finding in [8] is that while none of the correction methods gives a good blockage correction for different yaw angle conditions. The results for different correction equations are given in Table 2, for the purpose of comparison are the blockage effects obtained by the CFD approach. From the results shown in Table 2, it is seen that all the correction methods give the same trend for the corrections at different yaw angles, i.e., the blockage correction for the non-zero yaw angle is larger than zero yaw angle condition. This trend is in agreement with the blockage correction trend developed in CFD. The area ratio method, Maskell's method, Wall proximity, Hackett's and Thom & Herriot give consistently larger corrections. The comparisons further shows that, Mercker's method gives best agreement to CFD predictions, while the continuity method provides the best agreement to CFD predictions at 0° yaw angle.

Table 2: Blockage correction

Yaw angle (°)	0°	5°	10°
Continuity	0.128	0.151	0.192
Area ratio	0.033	0.039	0.049
Maskell	0.095	0.129	0.199
Wall proximity	0.077	0.085	0.099
Mercker	**0.107**	**0.156**	**0.235**
Hackett's	0.104	0.141	0.299
Thom & Herriot	0.119	0.143	0.190
$\Delta C_d\,(CFD)$	**0.132**	**0.176**	**0.266**

4.3 Wake Structure

To investigate the blockage effect, we visualized the flow structures over the near wake region by total pressure coefficient. Snapshots of wake structures around the rear-end of the vehicle at 0°, 5° and 10° yaw

angle are shown in Fig. 7, respectively. In baseline wind tunnel geometry simulation, it can be seen that the wake is more or less distorted by the presence of pressure gradients and wake is extended in the longitudinal direction as well as in the vertical direction. In ideal case simulation, the wake structure is not affected by the pressure gradients and wake is formed freely.

(a)

(b)

(c)

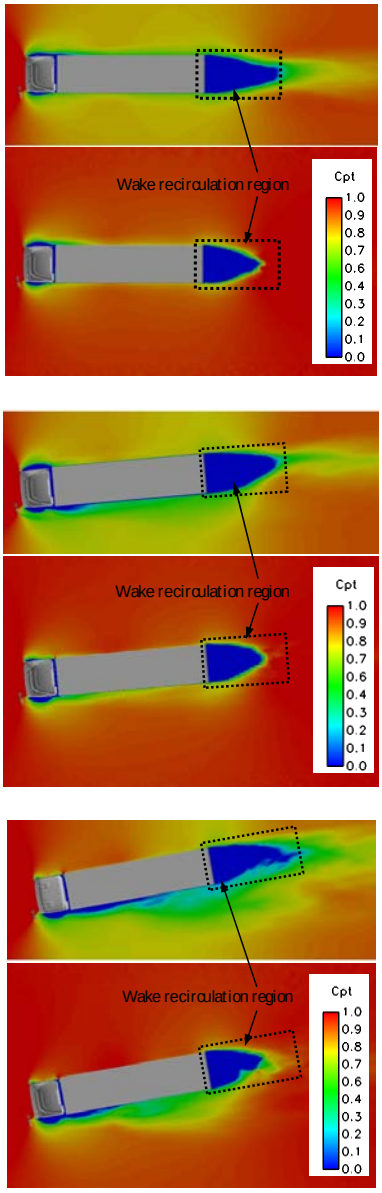

Fig. 7: Wake total pressure distribution, (a) 0°, (b) 5°, (c) 10° (Above: Baseline wind tunnel, Below: Ideal condition wind tunnel)

5. CONCLUSIONS

Computational fluid dynamics has been used to assess the closed-test-section wind tunnel blockage on real heavy duty truck model at different yaw angle conditions. All correction methods for aerodynamic drag show that poor agreement with CFD results except Mercker's method. The drag coefficients under the effect of yaw angle obtained with the correction method proposed recently by Mercker agreed well with the ideally obtained values at different yaw angles.

The numerical simulation reflects observations that the wind tunnel test approach is more accurate in evaluating the vehicle aerodynamic drag, and the CFD approach is less constraining in terms of the operating conditions of the virtual wind tunnel.

6. ACKNOWLEDGEMENTS

This work was supported by the Industrial Technology Research Grant Program in 2007 from the New Energy and Industrial Technology Development Organization (NEDO) of Japan. This study was conducted in a collaborative research project with Isuzu Advanced Engineering Center Ltd., and the geometry data and experimental data received are greatly appreciated.

7. REFERENCES

[1] K.R. Cooper et al. "Closed-Test-Section Wind TunnelBlockage Corrections for Road Vehicles", SAE International. SP-1176.

[2] Maskell, E.C. "A Theory of the Blockage Effects on Bluff Bodies and Stalled Wings in a Closed Wind Tunnel", ARC R&M 3400, Nov. 1963.

[3] E. Mercker et al. "The Influence of a Horizontal Pressure Distribution on Aerodynamic Drag in Open and Closed Wind Tunnels", SAE 2005-01-0867, 2005.

[4] E. Mercker. BMW AG, Germany and Dr. Koro Kitoh, Kozo Kitoh Technology. Inc, 2011: Private communication.

[5] Lock, C.N.H. "The Interference of a Wind Tunnelon a Symmetrical Body", ARC R&M 1275, 1929.

[6] Thom, A. "Blockage Corrections in a Closed High Speed Tunnel", ARC R&M 2033, Nov. 1943.

[7] Glauert, H. "Wind Tunnel Interference on Wings, Bodies and Airscrews", ARC R&M 1566, 1933.

[8] SAE Standard, '"Aerodynamic testing of road vehicles: closed-test-section wind tunnel boundary interference", SAE J2085, 1993.

9. NOMENCLATURE

Symbol	Meaning	Unit
C_d	Drag coefficient	(-)
F_d	Drag force	(N)
C_s	Lateral force coefficient	(-)
F_s	Lateral force	(N)
ρ	Air density	(kg/m^3)
A_M	Vehicle frontal area	(m^2)
A_N	Tunnel cross-section area	(m^2)
U_{inlet}	Inlet velocity	(m/s)
C_{DT}	Total drag coefficient	(-)
C_{Duw}	Measured drag coefficient	(-)
C_{Dw}	Corrected drag coefficient	(-)
G	Glauert factor	(-)